

Effect of Non-Magnetic Impurities (Zn, Li) in a Hole Doped Spin-Fermion Model for Cuprates

Charles Buhler¹, Seiji Yunoki² and Adriana Moreo¹

¹*Department of Physics, National High Magnetic Field Lab and MARTECH,
Florida State University, Tallahassee, FL 32306, USA*

²*Materials Science Center,
University of Groningen, Nijenborgh 4, 9747 AG Groningen, The Netherlands
(November 19, 2018)*

The effect of adding non-magnetic impurities (NMI), such as Zn or Li, to high-Tc cuprates is studied applying Monte Carlo techniques to a spin-fermion model. It is observed that adding Li is qualitatively similar to doping with equal percentages of Sr and Zn. The mobile holes (MH) are trapped by the NMI and the system remains insulating and commensurate with antiferromagnetic (AF) correlations. This behavior persists in the region $\%NMI > \%MH$. On the other hand, when $\%NMI < \%MH$ magnetic and charge incommensurabilities are observed. The vertical or horizontal hole-rich stripes, present when $\%NMI=0$ upon hole doping, are pinned by the NMI and tend to become diagonal, surrounding finite AF domains. The $\%MH$ - $\%NMI$ plane is investigated. Good agreement with experimental results is found in the small portion of this diagram where experimental data are available. Predictions about the expected behavior in the remaining regions are made.

PACS numbers: 74.62.Dh, 74.20.Mn, 71.10.Fd

Neutron scattering studies of the high-Tc cuprates have established that spin incommensurability (IC) appears in these compounds upon hole doping. [1] There is mounting evidence indicating that this IC is due to the formation of charge stripes. [2] One way of understanding the relationship between magnetic and charge fluctuations, as well as their impact in other properties of these materials, is by introducing NMI in the Cu-O planes. Some of these experimental results are puzzling. It has been observed that replacing Cu^{2+} by Zn^{2+} depletes antiferromagnetism without causing spin IC even at 25% doping. [3] It is estimated that an impurity content as large as 30-40% will be required to destroy AF order in this case. [4,5] While the addition of MH (Sr in $La_{2-x}Sr_xCuO_4$ (LSCO)) to lightly Zn-doped materials produces spin IC similar to the one observed in LSCO, [6] doping with Li, which introduces equal numbers of localized impurities and mobile holes does not induce spin IC at 10% Li doping of La_2CuO_4 (LCO). [7]

The goal of this paper is to gain theoretical understanding on the effect of NMI doping on cuprates. Numerical studies of Hubbard and t-J models, the Hamiltonians traditionally used to study the physics of the cuprates, are very difficult at low temperatures. A simpler spin-fermion model has been used successfully to understand magnetic and charge properties in these materials, showing that spin IC and charge stripe formation are related. [8] The spin-fermion model is constructed as an interacting system of electrons and spins, crudely mimicking phenomenologically the coexistence of charge and spin degrees of freedom in the cuprates. [9–11]. Its

Hamiltonian is given by

$$H = -t \sum_{\langle ij \rangle \alpha} (c_{i\alpha}^\dagger c_{j\alpha} + \text{h.c.}) + J \sum_i \mathbf{s}_i \cdot \mathbf{S}_i + J' \sum_{\langle ij \rangle} \mathbf{S}_i \cdot \mathbf{S}_j, \quad (1)$$

where $c_{i\alpha}^\dagger$ creates an electron at site $\mathbf{i} = (i_x, i_y)$ with spin projection α , $\mathbf{s}_i = \sum_{\alpha\beta} c_{i\alpha}^\dagger \boldsymbol{\sigma}_{\alpha\beta} c_{i\beta}$ is the spin of the mobile electron, the Pauli matrices are denoted by $\boldsymbol{\sigma}$, \mathbf{S}_i is the localized spin at site \mathbf{i} , $\langle ij \rangle$ denotes nearest-neighbor (NN) lattice sites, t is the NN-hopping amplitude for the electrons, $J > 0$ is an AF coupling between the spins of the mobile and localized degrees of freedom, and $J' > 0$ is a direct AF coupling between the localized spins. The density $\langle n \rangle = 1 - x$ of itinerant electrons is controlled by a chemical potential μ . Hereafter $t = 1$ will be used as the unit of energy. From previous phenomenological analysis the coupling J is expected to be larger than t , while the Heisenberg coupling J' is expected to be smaller. [10,11,8] The value of J will be here fixed to 2 and the coupling $J' = 0.5$, as in Ref. [8]. To simplify the numerical calculations, avoiding the sign problem, localized spins are assumed to be classical (with $|\mathbf{S}_i|=1$). This approximation is not as drastic as it appears and it was discussed in detail in Ref. [8]. The model will be studied using a Monte Carlo (MC) method, details of which can be found in Ref. [12]. Periodic boundary conditions (PBC) are mainly used but it has been checked that the results presented here are independent of the boundary conditions.

Doping with Zn will be simulated by randomly removing localized spins. This is achieved by turning $J = 0$ at the impurity site and $J' = 0$ along the four links that connect the impurity to neighboring sites. Li doping has

to be treated differently. Since it is in an oxidation state Li^+ (while Cu and Zn are $2+$), the ion effectively acts as a negative charge center. To simulate this effect the hopping t that connects the impurity to neighboring sites should be reduced. In addition, the Li ion is closed shell and thus, non-magnetic. This feature is simulated as in the case of Zn, by randomly removing localized spin degrees of freedom. An additional effect of Li doping is the introduction of one MH, thus the chemical potential has to be tuned such that the percentage of mobile holes equals the percentage of localized impurities.

To study the magnetic properties of the system the spin-spin correlation functions among the classical spins defined as $\omega(\mathbf{r}) = \frac{1}{N} \sum_i \langle \mathbf{S}_i \cdot \mathbf{S}_{i+\mathbf{r}} \rangle$ (where N is the number of sites) was measured. Its Fourier transform provides the spin structure factor $S(\mathbf{q})$. The momentum q_γ takes the values $2\pi n/L_\gamma$, with n running from 0 to $L_\gamma - 1$, and L_γ denoting the number of sites along the $\gamma=x$ or y direction.

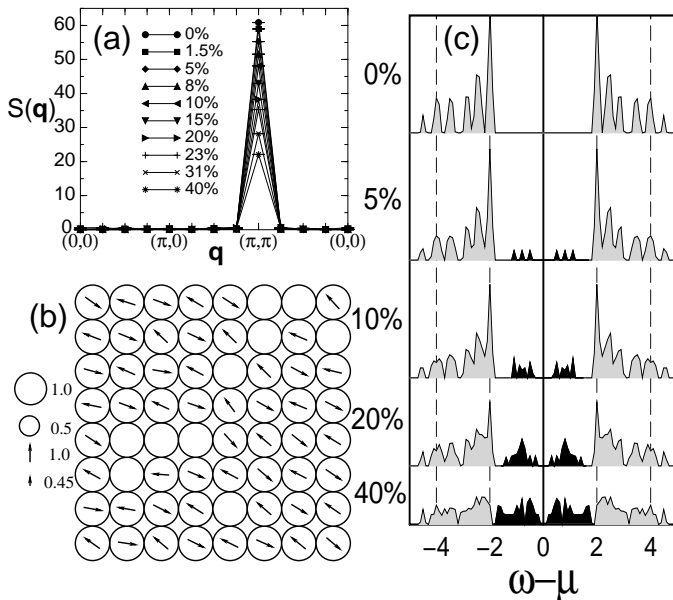


FIG. 1. (a) Structure factor $S(\mathbf{q})$ for the localized spins versus momentum, for $J=2$, $J'=0.05$ and $T=0.01$ on an 8×8 lattice and several Zn concentrations at $\langle n \rangle=1$ along $(0,0) - (0,\pi) - (\pi,\pi) - (0,0)$; (b) spin and charge distribution for a typical MC snapshot for 15% Zn and the same parameters as in (a). The arrow lengths are proportional to the projection of the localized spin on the (X-Z) plane, and the radius of the circles is proportional to the local electronic density $n(i)$, according to the scale shown. PBC are used. (c) Density of states for different percentages of Zn doping at $\langle n \rangle = 1$ with the same parameters as in (a). The dark areas indicate states with very little dispersion

In Fig.1-a the structure factor for different concentrations of localized NMI, like Zn, is shown for an 8×8 lattice at temperature $T = 0.01t$ and at $\langle n \rangle=1$ since doping with Zn does not modify the density of itinerant electrons. It can be seen that the peak remains at (π, π) for all the studied NMI concentrations. The only effect of

adding NMI is to reduce the intensity of the structure factor since spins are being removed. It is clear that random impurities do not destroy the AF order as can be observed from a snapshot at 15 % doping for the spins on the plane X-Z (Fig.1-b). The snapshot also shows a uniform charge distribution. This is in complete agreement with experimental data for Zn doping in LCO. [6] Our simulations can produce dynamical information directly in real-frequency without the need of carrying out (uncontrolled) analytic extrapolations from the imaginary axis. This allows us to study the behavior of the density of states (DOS). In Fig.1-c the DOS as a function of %NMI doping is presented. The addition of localized impurities creates states inside the gap which are indicated by a black filling in the figure. Analyzing the spectral functions $A(\mathbf{q}, \omega)$, it was observed that these states have very small dispersion which added to the absence of spectral weight at the chemical potential indicates that the system remains an insulator, in agreement with experiments. [3]

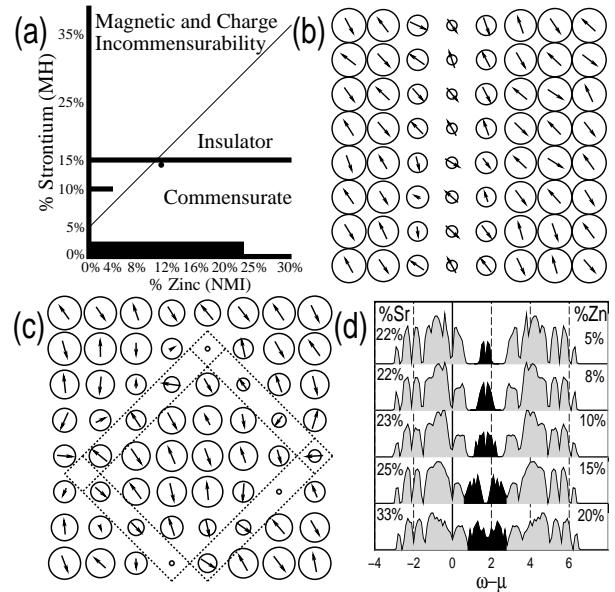


FIG. 2. (a) Schematic magnetic and charge phase diagram in the plane %Sr - %Zn. The thick lines and the dark areas indicate the regions that have been studied experimentally; (b) Spin and charge distribution for a MC snapshot on an 8×8 cluster for $J=2$, $J'=0.05$, $T=0.01$, at $\langle n \rangle \approx 0.85$ and % Zn=0. The spins are shown on the X-Y plane; (c) same as (b) but with % Zn=5; (d) DOS for different cases with %Sr > %Zn. The notation is as in Fig.1. PBC are used

The next step in our investigation is to study magnetic and charge properties varying both the mobile hole (Sr) and localized NMI (Zn) densities. In this case only a small fraction of the %Sr-%Zn plane has been explored experimentally. Studies were performed for $0 \leq \% \text{Zn} \leq 25$ and $0 \leq \% \text{Sr} \leq 3$ [4], $0 \leq \% \text{Zn} \leq 75$ and $\% \text{Sr} = 15$ [13], 12% Zn and 14% Sr [6], $0 \leq \% \text{Zn} \leq 12$ and 15% Sr [14], $0 \leq \% \text{Zn} \leq 4$ and 10% Sr [15], $0 \leq \% \text{Zn} \leq 40$ and

0% Sr [3]. Numerous experiments have also been performed on LSCO (without Zn). For $0 \leq \% \text{Sr} \leq 25$ neutron scattering experiments are presented in Ref. [16]. Zn-doped $\text{YBa}_2\text{Cu}_3\text{O}_{7-\delta}$ (YBCO) has also been studied with $0 \leq \% \text{Zn} \leq 4$ and the O content varying between 6.6 and 7, which roughly corresponds to a percentage of MH ranging between 9-15%. [17,15]. These regions are shown in Fig.2-a. In the same figure the magnetic and charge properties of the model Eq.(1) in the plane $\% \text{Sr} - \% \text{Zn}$ obtained from the present study are presented. In the absence of NMI, the addition of MH induces stripe formation, as well as spin IC. The stripes are either horizontal or vertical [8] and a snapshot for 15% MH and no localized impurities is shown in Fig.2-b. As it can be seen in the figure, the electronic density is depressed near the stripe indicating that perpendicular fluctuations are present, i.e., there is short range movement of holes in the direction perpendicular to the stripe.

When localized NMI are added they tend to trap holes. This reduces the effective hopping towards the impurity's nearest neighbor sites and diagonal stripes anchored by the impurities tend to develop as boundaries of AF domains. This effect is similar to the formation of diagonal stripes due to pinning experimentally observed. [18] An example of this behavior is shown in Fig.2-c where 3 NMI (i.e. 5% Zn) have been added to the system with $\langle n \rangle \approx 0.85$. A π -shift also occurs between the AF domains separated by the diagonal stripes. For some distributions of Zn impurities both diagonal and non-diagonal stripes, pinned by the impurities, coexist.

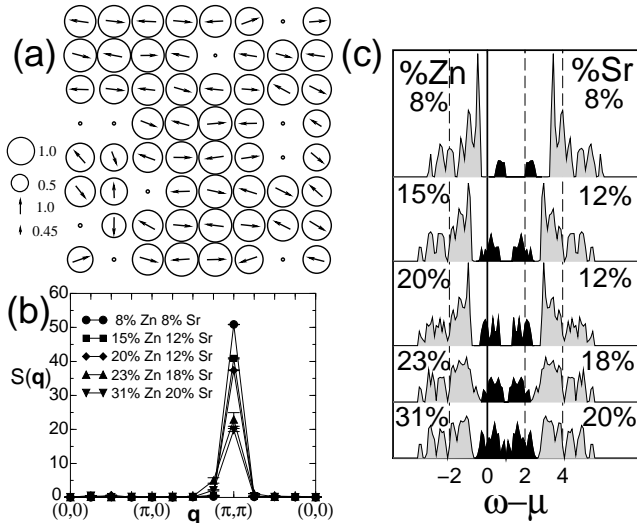


FIG. 3. (a) Snapshot for $\% \text{Zn} = \% \text{Sr} = 15$ in the plane X-Z; (b) $S(q)$ for different points with $\% \text{Zn} \geq \% \text{Sr}$; (c) Density of states for the parameters shown in (b). The parameters and notation are as in Fig.1

It has also been observed that while a localized impurity does not disturb the AF background, when the number of mobile holes is larger than the number of localized impurities a π -shift occurs in the x and y directions

across the impurity which eventually will give rise to spin IC (see Fig.2-c) [19,20]. According to this result, spin IC should be detected in the region $\% \text{Sr} > \% \text{Zn}$, more specifically, when the percentage of Sr is larger than that of Zn by approximately 5% according to experimental results for LSCO. This is in agreement with our observations if it is taken into account that due to the finite size of our system, spin IC is first detected when the peak in the structure factor is at $(\pi, 3\pi/4)$ and symmetrical points. Thus, it is here predicted that spin IC should be experimentally observed in samples with $\% \text{Sr} > \% \text{Zn}$. Notice that, due to the fact that the stripe structure is modified by NMI doping this may not be the same kind of IC observed in LSCO. In fact, it is possible that besides the magnetic peaks at $(\pi - \delta, \pi)$ and symmetrical points, less intense peaks may appear at $(\pi - \delta, \pi - \delta)$. More generally, as the percentage of NMI increases, IC peaks maybe observed in all directions in momentum space. The DOS indicates that in this situation the system has metallic characteristics although the chemical potential is in a pseudogap as shown in Fig.2-d. This feature is also in agreement with experiments. [21] A study of the spectral function shows that the states indicated with black, have very little dispersion. From the figure it can be seen that some mobile holes are trapped in these states and become almost localized but the extra mobile holes go into the dispersive states that form the pseudogap.

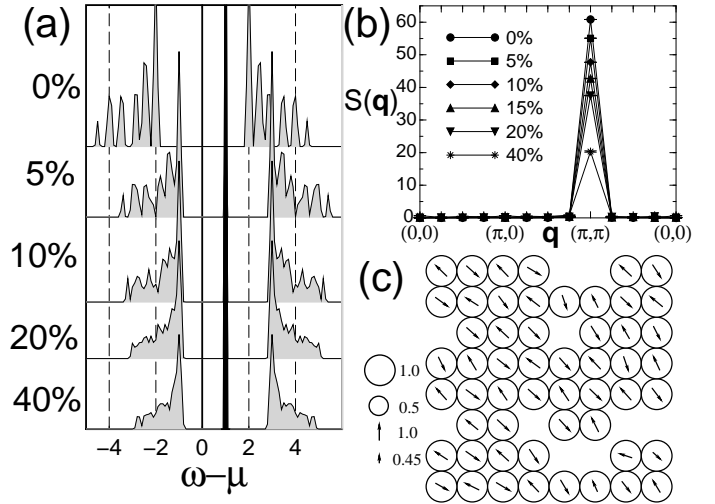


FIG. 4. (a) Density of states for different percentages of Li doping on an 8×8 cluster for $J=2$, $J'=0.05$, $T=0.01$; (b) Structure factor for the localized spins as a function of the momentum. The parameters are the same as in (a); (c) snapshot for $\% \text{Li} = 15$ (same parameters as in (a) and same notation as in Fig.1.)

When $\% \text{MH} \leq \% \text{NMI}$, the spinless centers tend to localize the mobile holes as it is shown in Fig.3-a for $\% \text{Zn} = \% \text{Sr} = 15$. Though the hopping towards the impurity sites is $t = 1$, the electrons prefer to stay away from that site, since the coupling J is zero and the observed

electronic density in them is just $\langle n_i \rangle \approx 0.03$, which indicates that the holes are very localized at the impurity sites. Notice that the hole localization, which is observed experimentally [13,4], appears naturally in our calculations, while it has to be assumed in other theoretical approaches. [22] The system is magnetically commensurate and the structure factor peaks at (π, π) as shown in Fig.3-b for different values of $\%Zn \geq \%Sr$. In these circumstances the system is an insulator as it can be seen in Fig.3-c where the DOS is displayed. When $\%Zn = \%Sr$ the chemical potential lies in a gap separating dispersive from non-dispersive states. When $\%Zn > \%Sr$ the chemical potential is located at the non-dispersive states. In both cases the system is an insulator. As mentioned before, very few experiments were performed in this region of the plane. However, our results are in agreement with the available data since insulating behavior was found for $\%Sr = 15$ and $\%Zn \geq 15$ Ref. [13] and $\%Sr = 3$ and $\%Zn \geq 3$ Ref. [4].

Note that the behavior observed along the line $\%Sr = \%Zn$ is in qualitative agreement with the experimental results available for Li doped LCO. It is well known that the system is an insulator up to the maximum possible percentage of Li (50%) [23,24] and at 10% doping spin IC is not observed [7] which was very unexpected. Thus, these results indicate that qualitatively, Li doping should be equivalent to equal percentages of Zn and Sr doping. However, in order to represent Li doping more accurately, it has to be considered that Li is less positively charged than Zn and Cu and thus it should act as an attractor of mobile holes. To mimic this behavior the hopping towards the impurity sites should be reduced. In our previous results it has been observed that $t=1$ tends to greatly localize the mobile holes since the electronic density at the impurity sites is only 0.03. Thus, any smaller value of t will not introduce important qualitative changes but, for completeness, and since it has been used in other approaches, [22] the results for $t=0$ near NMI are also presented. In this case the MH get trapped by the impurity and become totally localized. This can be seen in Fig.4-a where the density of states is shown for different percentages of Li doping. Localized states (marked in black), which do not disperse with momentum, proportional to the number of added holes appear in the density of states, and the chemical potential lies inside a gap indicating that the system is insulator as experimentally found. [25,24]. Incommensurability is not observed as it can be seen in Fig.4-b where the structure factor is displayed. A snapshot is presented in Fig.4-c.

Summarizing, the effect of adding non-magnetic impurities to a model of interacting fermions and classical spins has been investigated using MC techniques. When the percentage of mobile holes is larger than the NMI, charge and spin IC is observed. The NMI act as pinning centers for the horizontal and vertical stripes that are observed in the absence of vacancies. The pinned stripes tend to become diagonal and surround AF domains. Thus, the observed incommensuration may not

be identical to the one observed in LSCO. When the percentage of MH is equal to or smaller than the NMI, the mobile holes are trapped by the impurities and the system remains insulator and magnetically commensurate. Thus, based on our study, it is predicted that incommensuration should not be experimentally observed in this situation, and that samples with equal percentages of Sr and Zn should behave similarly to the Li doped ones.

A.M. is supported by NSF under grant DMR-9814350. Additional support is provided by the National High Magnetic Field Lab and MARTECH.

-
- [1] S-W. Cheong *et al.*, Phys. Rev. Lett. **67**, 1791 (1991); P. Dai *et al.*, Phys. Rev. Lett. **80**, 1738 (1998); H.A. Mook *et al.*, Nature **395**, 580 (1998).
 - [2] J.M. Tranquada *et al.*, Phys. Rev. Lett. **78**, 338 (1997).
 - [3] A. Chakraborty *et al.*, Phys. Rev. **B40**, 5296 (1989); G. Xiao *et al.*, *ibid.* **42**, 240 (1990); K. Uchinokura *et al.*, Physica **B 205**, 234 (1995).
 - [4] M. Hücker *et al.*, Phys. Rev. **B59**, R725 (1999).
 - [5] S-W. Cheong *et al.*, Phys. Rev. **B44**, 9739 (1991).
 - [6] K. Hirota *et al.*, Physica **B 241-243**, 817 (1998).
 - [7] W. Bao *et al.*, to appear in PRL. Preprint, cond-mat/9909256.
 - [8] C. Buhler *et al.* Phys. Rev. Lett. **84**, 2690 (2000).
 - [9] P. Monthoux *et al.*, Phys. Rev. **B47**, 6069 (1993); A. Chubukov, Phys. Rev. **B52**, R3840 (1995); S. Klee and A. Muramatsu, Nucl. Phys. **B 473**, 539 (1996).
 - [10] J.R. Schrieffer, J. of Low Temp. Phys. **99**, 397 (1995); B.L. Altshuler *et al.* Phys. Rev. **B52**, 5563 (1995).
 - [11] C.-X. Chen *et al.* Phys. Rev. **B43**, 3771 (1991).
 - [12] E. Dagotto *et al.*, Phys. Rev. **B 58**, 6414 (1998).
 - [13] G. Hilscher *et al.*, Z. Phys. **B72**, 461 (1988).
 - [14] K. Karpinska *et al.*, preprint cond-mat/9911149.
 - [15] Y. Fukuzumi *et al.*, Phys. Rev. Lett. **76**, 684 (1996).
 - [16] K. Yamada *et al.*, Phys. Rev. **B57**, 6165 (1998).
 - [17] W.A. MacFarlane *et al.*, preprint, cond-mat/9912165; Y. Sidis *et al.*, preprint, cond-mat/9912214; K. Segawa and Y. Ando, Phys. Rev. **B 59**, R3948 (1999); H.F. Fong *et al.*, Phys. Rev. Lett. **82**, 1939 (1999).
 - [18] J.M. Tranquada *et al.*, Phys. Rev. **B 54**, 7489 (1996).
 - [19] Since PBC are used the π -shift is not observed when it would cause spin frustration. [8]
 - [20] G. Martins *et al.*, preprint.
 - [21] T. Sato *et al.*, preprint, to appear in Phys. Rev. Lett.
 - [22] A.H. Castro Neto and A.V. Balatsky, cond-mat/9805273; G. Martins *et al.*, Phys. Rev. Lett. **78**, 3563 (1997).
 - [23] Y. Yoshinari *et al.*, Phys. Rev. Lett. **77**, 2069 (1996).
 - [24] B.J. Suh *et al.*, Phys. Rev. Lett. **81**, 2791 (1998).
 - [25] M. Kastner *et al.*, Phys. Rev. **B37**, 111 (1988); J. Sarrao *et al.*, Phys. Rev. **B54**, 12014 (1996).